nature neuroscience

Encoding a temporally structured stimulus with a temporally structured neural representation

Stacey L Brown, Joby Joseph & Mark Stopfer

Sensory neural systems use spatiotemporal coding mechanisms to represent stimuli. These time-varying response patterns sometimes outlast the stimulus. Can the temporal structure of a stimulus interfere with, or even disrupt, the spatiotemporal structure of the neural representation? We investigated this potential confound in the locust olfactory system. When odors were presented in trains of nearly overlapping pulses, responses of first-order interneurons (projection neurons) changed reliably, and often markedly, with pulse position as responses to one pulse interfered with subsequent responses. However, using the responses of an ensemble of projection neurons, we could accurately classify the odorants as well as characterize the temporal properties of the stimulus. Further, we found that second-order follower neurons showed firing patterns consistent with the information in the projection-neuron ensemble. Thus, ensemble-based spatiotemporal coding could disambiguate complex and potentially confounding temporally structured sensory stimuli and thereby provide an invariant response to a stimulus presented in various ways.

Visual[1–4], auditory[5–7], tactile[8–10], and olfactory[11–15] senses all use temporal coding mechanisms[16] for which the timing, rather than just the rate, of action potentials is important for the neural representation of the stimulus[17,18]. If a neural response pattern significantly outlasts the stimulus, new stimuli might arrive before the response to a previous stimulus is complete[19]. This situation is particularly interesting in olfaction; in principal neurons, odor pulses can elicit response patterns that endure beyond the pulse's offset[11,14] and, further, natural odor plumes can have repeated, rapid and nearly overlapping encounters with olfactory receptors[20]. Given these potential confounds, how can neural systems use spatiotemporal representations to encode and decode temporally structured stimuli?

In the locust, projection neurons in the antennal lobe—the analogs of vertebrate mitral cells[21]—respond to odors with complex spiking patterns that consist of epochs of excitation, inhibition and quiescence. These patterns vary with odor identity and concentration, and can greatly outlast the odor receptor neurons' encounter with the odor[11,14]. The antennal lobe's network of excitatory projection neurons and inhibitory local neurons generates these firing patterns when driven by input from olfactory receptor neurons[22,23]. These spiking patterns, distributed broadly across the projection neuron population, are parsed into brief segments by odor-evoked oscillations and are read by downstream follower neurons (the Kenyon cells) which receive convergent input from many projection neurons[15,24] (R.A. Jortner and G. Laurent, *Soc. Neurosci. Abstr.* **412**, 21, 2004). The oscillating projection neuron ensemble, through feed-forward inhibition, generates brief integration windows in the Kenyon cells[24]. Kenyon cells respond to odors with very sparse spiking, often demonstrating great specificity with respect to odors and even particular concentrations of odors[25,26].

Here we examine how the locust olfactory system responds to very short (100-ms) repeated odor pulses; the timing was chosen to approximate that observed in natural odor plumes[20]. In a turbulent environment, odor is carried in an intermittent fashion in the form of filaments of odor-laden air that vary in concentration, duration and frequency with which they appear. These factors are modulated by wind speed, amount of turbulence, delivery mechanism and distance from the odor source[20,27]. We selected stimulus parameters on the basis of odor plume measurements made outdoors, in which filaments were observed to encounter a sensor in a series of bursts that averaged about 100 ms in duration and arrived, on average, at approximately 500-ms intervals[20].

We made intracellular recordings from projection neurons and extracellular tetrode recordings from projection neurons and Kenyon cells in adult locusts. We delivered brief (100-ms) odor pulses in trains of 3 or 10 pulses; inter-pulse intervals ranged from 500 to 1,250 ms but were constant within a train. For each pulse pattern, we delivered blocks of 10 trials (15–30 s inter-trial interval), with the blocks given in random order. We used a variety of odorants and concentrations (see Methods).

Our results showed that ensemble-based coding mechanisms can disambiguate complex and potentially confounding temporally structured sensory stimuli, thus providing an invariant response to a stimulus presented in different ways while preserving information about the stimulus timing.

RESULTS

Projection neuron responses vary with odor pulse pattern

For most odor–projection neuron combinations, the number of spikes elicited by odor pulses changed reliably, and sometimes substantially, with pulse position, because lengthy responses to one pulse interfered

National Institute of Child Health and Human Development, US National Institutes of Health, Building 35, Room 3A-102, Bethesda, Maryland 20892, USA. Correspondence should be addressed to M.S. (stopferm@mail.nih.gov).

Received 15 August; accepted 19 September; published online 16 October 2005; doi:10.1038/nn1559

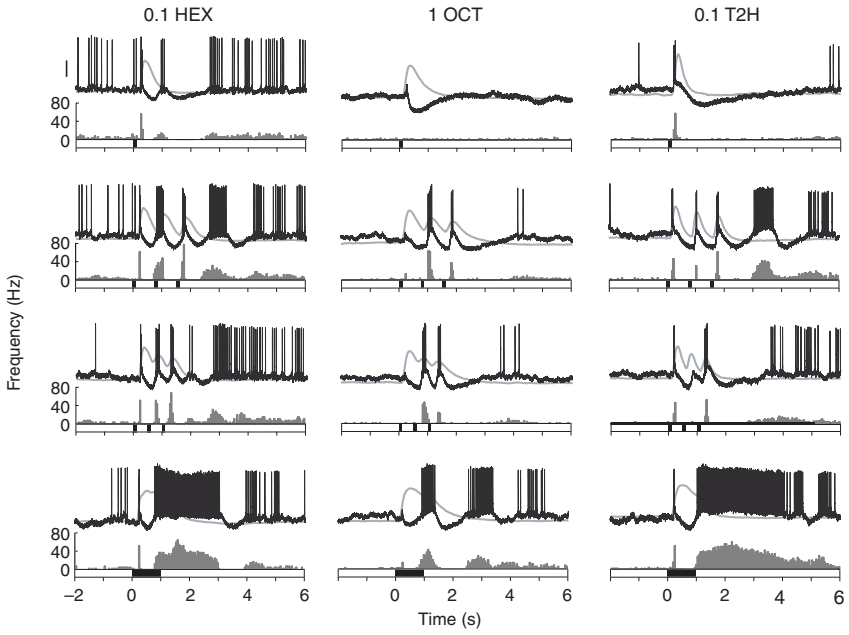

Figure 1 The responses of projection neurons change with odor and inter-pulse intervals. Rapid trains of odor pulses evoked responses that interfered with one another (see text). Example of a projection neuron (intracellular recording), responding to three odors (columns) presented in four patterns (rows). Black bars on abscissa: odor presentation times. Gray histograms, responses to ten consecutive trials exemplified by the intracellular trace; gray lines, simultaneous EAG recordings indicating afference from the antenna; note that the responses of the projection neurons may outlast this afference. Top row, single 100-ms pulse; second row, train of three 100-ms pulses with a 1,250-ms IPI; third row, train of three 100-ms pulses with a 500-ms IPI; bottom row, single 1,000 ms pulse. Scale bar, 10 mV. 0.1 HEX, diluted hexanol; 1 OCT, octanol; 0.1 T2H, diluted *trans*-2-hexen-1-ol.

with responses to subsequent pulses. We recorded intracellularly from 211 projection neurons (in 92 experiments) and extracellularly (with tetrodes) from 117 projection neurons (in 14 experiments) and 67 Kenyon cells (in 10 experiments). In a typical intracellular recording (**Fig. 1**), the projection neuron responded reliably to a single, brief pulse of diluted (0.1) hexanol (see Methods) with a quick burst of spikes which was followed by another, smaller burst and a lengthy hyperpolarization. The projection neuron also spiked reliably in response to each of the pulses in a three-pulse train (with inter-pulse intervals, IPIs, of 500 ms and 750 ms). Note that the electroantennogram (EAG) response decreased in amplitude over the pulse trains, probably indicating olfactory receptor adaptation; this recovered within seconds, before the next trial. For another odorant (1 octanol), single pulses elicited only inhibition, whereas trains of three pulses reliably elicited spikes for the second and third pulses (but not the first). For 0.1 *trans*-2-hexanol, single pulses and trains with a 750-ms IPI elicited reliable spiking, whereas trains with the 500-ms IPI elicited reliable spiking only for the first and third pulses (but not the second). Responses to trains of odor pulses often included strong and reliable bursts of spikes after the last pulse; these 'after-responses' became longer and more intense as the duration of individual odor pulses increased (see, for example, **Fig. 1**, bottom, 1-s odor pulse). The timing and intensity of excitatory and inhibitory odor response components in this projection neuron reflected multiple underlying mechanisms (see Discussion) and determined how closely the bursts of spikes could track each separate odor pulse within a train.

We obtained similar results from extracellular recordings made simultaneously from multiple projection neurons (**Fig. 2**). Different

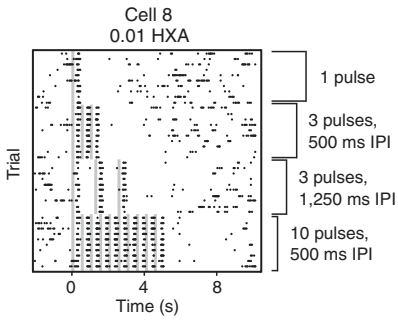

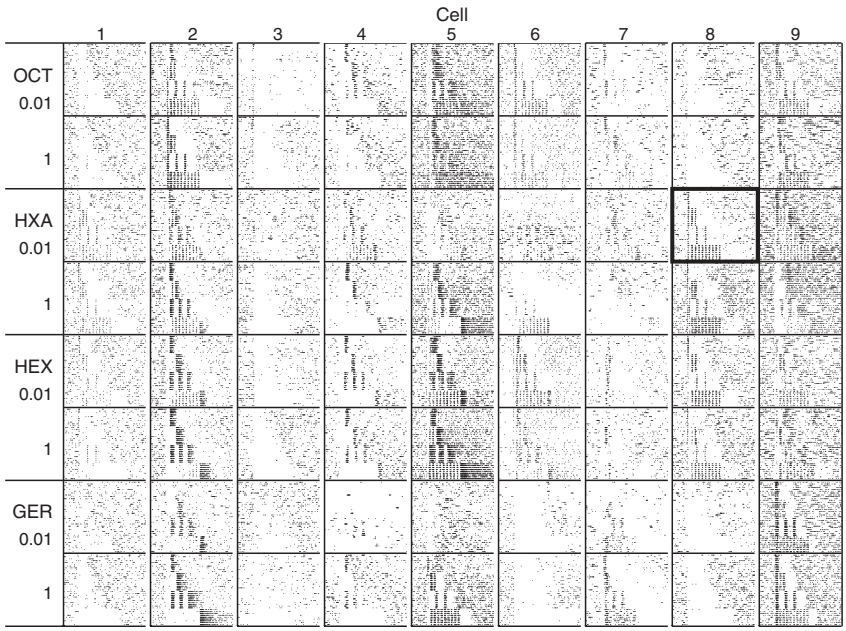

Figure 2 The responses of projection neurons to odors and the extent of interference between overlapping responses patterns vary greatly depending on the odor and the cell. Spike-time raster plots show simultaneous extracellular recordings from nine projection neurons, in response to four odor-pulse delivery patterns (ten trials each) for four odorants, each at two concentrations. Inset, enlarged example of a particular combination of odor and projection neuron. Gray bars indicate odor delivery times. Stimuli were delivered in random order but are organized here in the sequence shown in the inset. Note the variety of responses observed in different projection neurons and to different odors and concentrations.

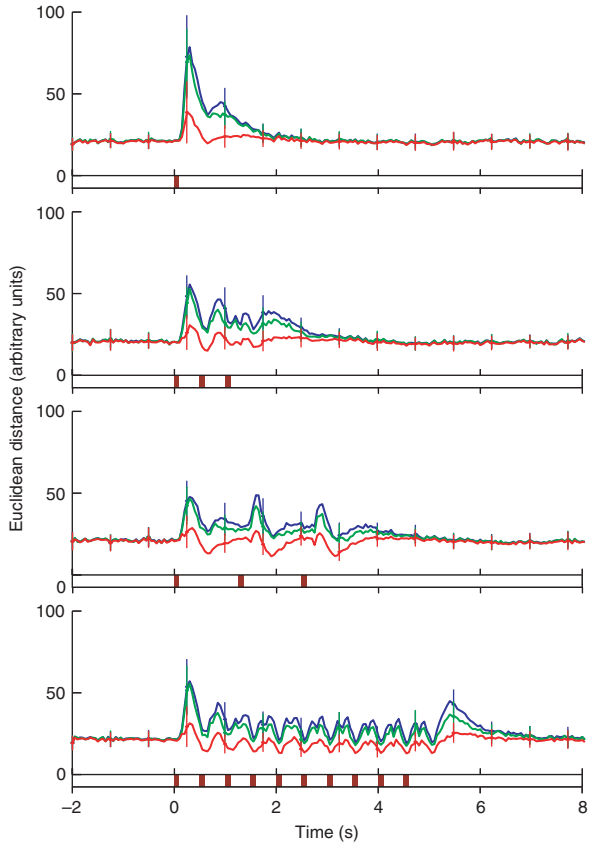

Figure 3 Over time, the responses of projection neurons varied more across odors and concentrations than across trials. The average Euclidian distance (see text and Methods) for every 50-ms snapshot of the projection-neuron ensemble response is shown for each of the odor pulse patterns tested (indicated by red bars on the abscissa). In the ensemble response over time, repeated trials of the same odor and concentration elicited small variations from the baseline (red line), whereas trials with changes in concentration of the same odor (green) or changes of odors at the same concentrations (blue) elicited, respectively, larger variations from the baseline and from each other. From top: single 100-ms pulse; three pulses with a 500-ms IPI; three pulses with a 1,250-ms IPI; ten pulses with a 500-ms IPI. Error bars, s.d.

projection neurons responded in different ways to the same stimulus pulses. In some neurons, spikes elicited by some odors faithfully tracked every pulse in a train (see, for example, the response of cell 8 to 0.01 hexanal, **Fig. 2** inset); however, this was atypical, and such a projection neuron responded differently when the animal was presented with a different odor (see cell 8's response to 1 OCT). None of the 117 projection neurons in our extracellular set were able to reliably track the pulse timing of all odor-concentration combinations.

Of the 936 odor–projection neuron combinations in our set, 719 elicited spikes. For most of these combinations, the number of spikes generated varied significantly ($P < 0.05$; see Methods) with pulse position: 59% showed significant changes over three pulses with a 500-ms IPI, and 68% showed significant changes over ten pulses with a 500-ms IPI. In about one-third of the cases in which spikes were elicited, the changes were substantial. For example, 10% of the odor–projection neuron combinations resulted in spiking in response to only the first pulse; 10% to all but the first pulse; 7% to only the last pulse; and 3% to all but the last pulse. Thus, for most projection neurons, the temporal structure of the odor interfered with the temporal structure of its neural representation.

Analyzing responses of an ensemble of projection neurons

Multiple projection neurons converge onto their follower neurons (which include Kenyon cells; R.A.J. and G.L., *Soc. Neurosci. Abstr.* **412**, 21, 2005), and odors are represented by spiking activity distributed across ensembles of projection neurons[11,14]. We considered that, despite the interference-induced variability observed in the responses of individual projection neurons, invariant properties of the stimulus might emerge at the ensemble level. Thus, we pooled our set of extracellularly recorded projection neurons so as to approximate a portion of the projection-neuron population found in the antennal lobe (see Methods) and then examined the set's information content.

We sought to analyze the projection-neuron ensemble response as it evolved during and after each stimulus presentation. Therefore, we binned the firing patterns of each projection neuron into brief (50-ms or 100-ms) time segments and then constructed, for each time segment, a separate response vector consisting of the binned firing of each of the 117 projection neurons[26]. Thus, each vector had 117 elements and represented a 'snapshot' of the transient coactivity of projection neurons in the ensemble at a given point in time. This technique allowed us to make rigorous comparisons between responses. The vectors could be treated as points within a 117-dimensional response space; the Euclidean distance between these points provided a measure of the similarity of the response patterns. By considering a series of vectors representing consecutive points in time, we were able to compare responses as they evolved. We found that (as is already evident from the examples in **Figs. 1** and **2**) the responses were reliable (**Fig. 3**): (i) repeated trials with the same odor and concentration elicited

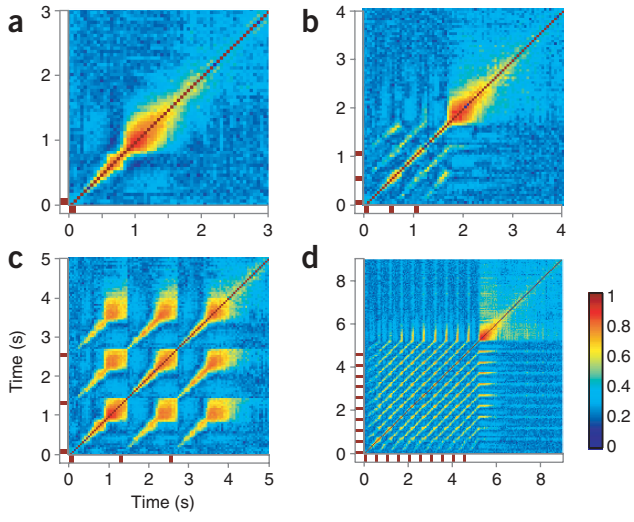

Figure 4 Cross-correlations indicate that the response of the projection-neuron ensemble evolves gradually over the duration of the response. (**a–d**) For each delivery pattern of the 1 hexanol odorant, the cross-correlation coefficients ($P < 0.001$; see Methods) were calculated between consecutive 50-ms bins of the ensemble response. The cross-correlations obtained from other odorants were similar. Comparing the response to a single pulse with itself over time shows a correlated region between 150- and 300-ms wide, indicating that the subset of projection neurons active during the response evolves gradually. Also, responses to any given pulse in a train were highly correlated with other responses to pulses in that train. Red bars, odor pulse times. (**a**) Single 100-ms pulse; (**b**) three pulses with a 500-ms IPI; (**c**) three pulses with a 1,250-ms IPI; (**d**) ten pulses with a 500-ms IPI. Note the different time scales.

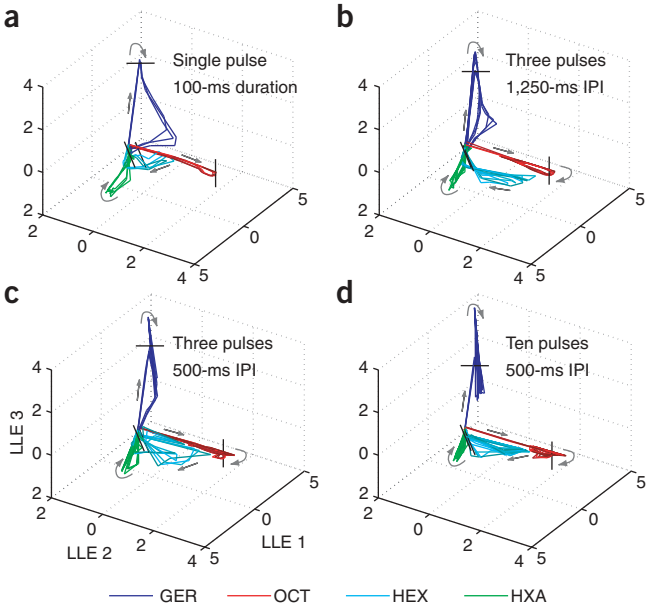

Figure 5 Visualization of the projection-neuron ensemble responses over time reveals invariant odor-specific trajectories, regardless of odor delivery pattern. (**a–d**) Different odor delivery patterns; colors indicate different odorants. The trajectories, describing the evolution of the ensemble response over time, return to the same areas of response space over repeated trials and remain in the same orientation, regardless of odor delivery pattern. The longer IPI allows the trajectory to return to the spontaneous state after each pulse; however, the shorter IPI causes the trajectories to loop away from the spontaneous state within the odor space. Three-dimensional embedding using LLE was computed for each time point (100-ms bins), for 5 s from the onset of the first odor pulse, averaged over three trials. Consecutive time points were joined together to form distinct trajectories for each odor response. Short black lines indicate the trajectory point 0.5 s after the onset of the stimulus; gray arrows indicate the direction of the trajectory over time. GER, geraniol; OCT, octanol; HEX, hexanol; HXA, hexanal. For clarity, only responses to the higher concentration of each odor are shown here; the response trajectories for the lower concentration were shorter but occupied the same manifolds as did the higher ones. (High- and low-concentration response trajectories are shown together in **Supplementary Fig. 2**.)

responses that were similar to one another; (ii) changing the odor concentration elicited response patterns that quickly began to differ from baseline and also from patterns elicited by different concentrations; and (iii) changing the odor identity elicited response patterns that were even further from baseline and from each other.

The patterns of activity elicited by the odorants changed gradually during and after the stimulus for any given coactivity snapshot, ensemble responses were highly and significantly correlated with the responses obtained from snapshots before and after it as is evident in the correlation plots (**Fig. 4a**). Further, responses to multiple odor pulses were highly and significantly correlated with each other (**Fig. 4b–d**). Notably, relatively abrupt changes in correlation occurred during the pulse trains, as new responses appeared to truncate ongoing responses (**Fig. 4b–d**).

Visualizing ensemble responses to odor pulses

To visualize the gradually evolving ensemble responses, we first reduced the dimensionality of the snapshot vectors using local linear embedding (LLE), a technique suitable for high-dimensional, nonlinear and gradually changing data[26,28] (see Methods). Then, we plotted the first three dimensions so as to obtain a series of points that, when joined in sequence, formed a trajectory representing the response over time to each odor presentation (**Fig. 5**).

Single, brief pulses of odorant elicited simple response trajectories looping away from, and then back to, the rest point (**Fig. 5a**). These trajectories were constructed by sampling, in brief time bins, the firing patterns of the projection-neuron ensemble; thus they illustrate the fact that gradually changing subgroups of projection neurons within the ensemble were transiently coactive during and after the odor presentation. Trajectories representing repeated trials were superimposable, which indicates that ensemble responses were reliable and reproducible. The trajectories elicited by different odorants looped through separate regions of the response space because different odors transiently activated different subgroups of projection neurons within the ensemble. Also, we found that each odor pulse within a train, regardless of the IPI, elicited a trajectory that looped through and re-circled the same odor-specific regions of response space as did the single odor pulse (**Fig. 5b–d**). The response of the projection-neuron ensemble, considered piecewise, was odor specific and invariant with respect to the odor-pulse pattern.

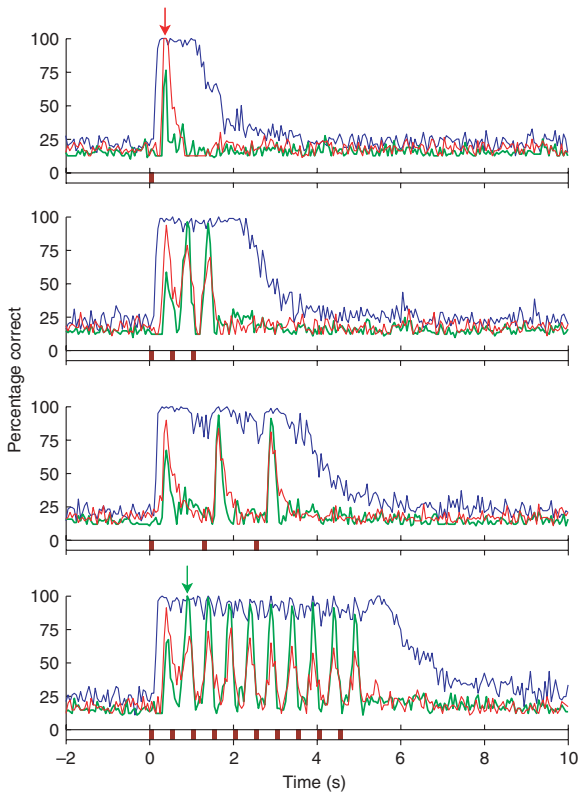

Figure 6 Ensemble responses are well classified, regardless of odor delivery pattern. Any given 50-ms template could effectively classify the odors. Blue line, result of an unsupervised classification algorithm applied separately to every 50-ms time bin for all the different odor delivery patterns (red bars on abscissa). Chance level, 12.5%. Classification success exceeded 80% throughout, independent of the pulse sequence. Red and green lines indicate classification performance obtained by applying a single 50-ms bin 'template.' Arrows indicate the templates (red, from the single pulse; green, from the second in the train of ten pulses). Classification success far exceeded chance for all delivery patterns and registered a peak at the time of each odor pulse.

The existence of odor-specific, transiently coactive subgroups of projection neurons (as revealed by the distance, correlation and trajectory analyses) suggested that the responses should contain sufficient information about the odorants to allow the stimulus to be effectively classified—even given only brief snapshots of time. Indeed, we found that a simple, unsupervised classification algorithm, using only the eight most significant dimensions in the dataset (see Methods), could effectively distinguish the eight odor-concentration combinations from one another; using any given 50-ms time bin during the odor response, the algorithm was successful at classifying the odors (80–100% classification success), regardless of the pulse pattern (**Fig. 6**). Thus, the information available in any brief snapshot of the ensemble response is sufficient to classify the odors, independent of their temporal presentation characteristics.

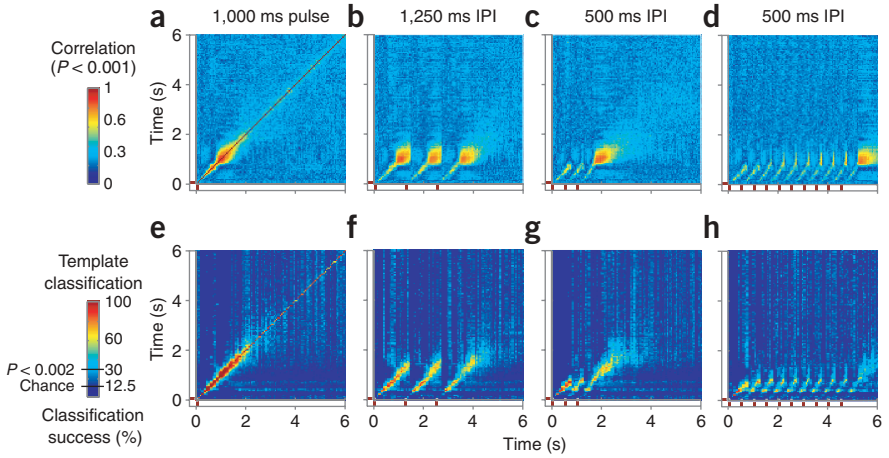

Figure 7 Correlation and classification analyses show that responses to single odor pulses are comparable to responses during odor pulse trains. (**a**–**h**) Correlation (**a**–**d**) and classification (**e**–**h**) analyses, comparing responses to single pulses (ordinate) to responses to trains of three or ten pulses (abscissa) over time, show common response features regardless of the odor presentation pattern. The common features (subgroups of transiently coactive projection neurons) allow for high levels of successful response classification, particularly during the onsets and offsets of responses. Correlations shown are significant ($P < 0.001$). Classification probabilities were determined as described in Methods and in **Supplementary Figure 5**. Red bars on axes represent odor pulse times.

Recognizing time-varying features of the odor stimulus

However, the evolving trajectories indicate gradual, continuous changes in the composition of odor-specific sets of transiently coactive projection neurons. This raises interesting questions: (i) if odor recognition requires the matching of a transient stimulus-elicited activity pattern with a stored template, do many different templates—each representing different points along the trajectory—need to be stored?; and (ii) does a template representing one odor-presentation pattern match the projection-neuron ensemble activity created by a different presentation pattern of the same odorant?

We found that projection-neuron ensemble responses evoked by one presentation pattern were highly and significantly correlated with the responses evoked by the same odorant presented in a different pattern (**Fig. 7a–d**). This suggests that cross-classification should be successful. We then used our projection-neuron activity vectors as templates, each template representing a 50-ms snapshot of the ensemble activity evoked by different odors presented in different patterns. We tried to classify responses evoked by one presentation pattern using responses evoked by the other patterns (**Fig. 7e–h**). The resulting template classification diagram for single, brief (100-ms) odor pulses reveals an evolving series of useful templates (**Fig. 7e**)—no single time bin was optimally effective during and after the stimulus. However, because the ensemble response patterns evolved gradually, any given 50-ms template could effectively classify much longer (150–300 ms-long) portions of the response.

When we applied the template sequence formed from the single pulse to the responses evoked by a widely spaced (1,250-ms IPI) train of three pulses, a similar effect emerged (**Fig. 7f**): odors were successfully classified throughout the responses—although with the greatest success during the first part of each response. When the single-pulse template was applied to a three-pulse train with a shorter (500-ms) IPI, classification was again successful throughout the responses, but this time the best classification occurred at the beginning and the end of

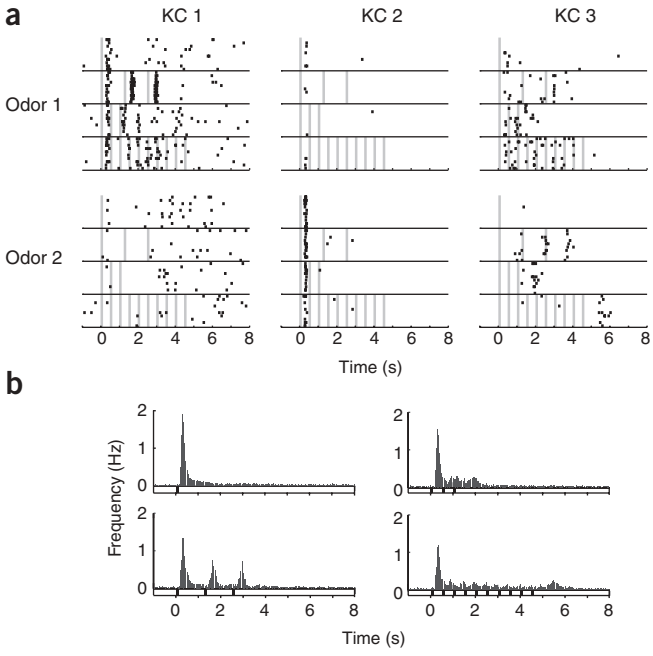

Figure 8 Kenyon cells fire sparsely throughout the odor responses. (**a**) Examples of Kenyon-cell responses to different odors and presentation patterns. Individual Kenyon cells revealed preferences for odors and response times. KC 1 and KC 2 were recorded simultaneously; odor 1: 1 octanol; odor 2: *trans*-2-hexen-1-ol. For KC 3, odor 1: 1 octanol; odor 2: 1 hexanol. KC 1 responded to most presentations of one odorant regardless of presentation pattern, but did not respond to a different odorant. KC 2 responded reliably but exclusively to the onset of an odor pulse or train for one odorant, but did not respond to other odorants. Finally, KC 3 responded to both odorants, although with differently timed responses for each, firing throughout odor 1, but only during the 'after-response' of odor 2. (**b**) Histograms of the firing frequencies, over time, of all 67 examined Kenyon cells, shown for each odor delivery pattern. Spiking occurred throughout the odor response but was most frequent at the beginning.

each pulse in the series (**Fig. 7g**). The arrival of each new pulse seemed to truncate the period of classification success, because the onset responses differed from the offset responses; however, the last pulse of the train elicited a lengthy offset response that matched the offset of the single pulse. The response to a ten-pulse train with a 500-ms IPI effectively matched the response to the single pulse, mainly during the train's onset but also at other times during each of the ten pulses (**Fig. 7h**). We obtained similar results from all possible cross-classification matches (data not shown).

Thus, a single stored 50-ms template was sufficient for recognizing the ensemble-wide activity patterns evoked by an odorant, regardless of the odorant's presentation pattern (**Fig. 6**); by tracking the template-matches over time, we were able to obtain a description of the time-varying features of the stimulus (its odor, concentration and timing pattern). Multiple templates, if available, could serve to distinguish and recognize the onsets of pulses of a given odor.

Responses of downstream neurons to odor pulses

Our analysis of the ensemble response was based on the integration properties of the projection-neuron followers, the Kenyon cells. Thus, our analysis leads to predictions for Kenyon cell behavior. Because different subsets of projection neurons were coactivated by different odors and because these subsets converge onto Kenyon cells, we expected the responses in some Kenyon cells to be odor specific. Further, because the projection-neuron subsets that were coactive during the brief Kenyon cell integration window continuously changed during the odor response, we expected that Kenyon cells would respond to different odors at different times during this evolution. Also, because the ensemble response patterns elicited by trains of odor pulses tended to repeat with each pulse (that is, the trajectories re-circled portions of the same response space), we expected that the Kenyon cells would respond at particular times during the odor trains. Our recordings from Kenyon cells confirmed these predictions (**Fig. 8**), showing that individual Kenyon cells can respond with some specificity to different odors and to different temporal features of an odor presentation. Taken collectively, the data show that the Kenyon cells responded throughout the ensemble response but most prominently during response onset.

DISCUSSION

We examined how a temporally structured stimulus is encoded by a temporally structured distributed neural representation. The responses of individual first-order interneurons (projection neurons in the locust antennal lobe) indicated that the two types of temporal structures significantly interfered with each other. However, this potential confound was resolved by considering the responses of these neurons in the context of their ensemble activity; this activity was sufficiently informative to allow the accurate detection and classification of the invariant properties of the stimulus and its temporal structure. Second-order 'decoder' interneurons (Kenyon cells) responded as predicted on the basis of the information available in the first-order ensemble response.

Spatiotemporal coding mechanisms—including those subserving vision[1–4], audition[5–7], touch[8–10] and olfaction[11–15]—are common in neural systems. In most cases, neural responses are brief (although some neurons, such as those in inferior temporal cortex, show sustained firing following brief visual stimuli[1]) and seem to track the stimuli closely. The potential for confounds between temporally structured stimuli and their neural representations seems greatest in olfaction, where the response duration in principal neurons often outlasts the odor stimuli[11,14,15].

Olfactory receptor neurons in insects can follow rapid odor-pulse trains[29–32] precisely; in particular, macroglomerular projection neurons, specialized for pheromone detection, have been shown to track the timing of pheromone plumes reliably[33–35]. Some insects, for example, seem to use this information when moving toward pheromone sources[36–38]. However, non-pheromonal afferent activity that is relatively stimulus locked is reformatted by the circuitry of the antennal lobe into complex spatiotemporal activity patterns distributed across the population of projection neurons[11,15,22,26,39]. These activity patterns, which vary with—and thus contain information about—odor identity and concentration (**Figs. 1** and **2**), are further parsed into a series of gradually evolving snapshots, roughly 50 ms long, by an oscillatory synchronization mechanism driven by the circuitry of the antennal lobe[24]. Projection neurons provide the only pathway for olfactory information from the antennal lobe to reach other neural targets, including the Kenyon cells. The locust antennal lobe contains about 830 projection neurons[19]; recent results suggest that more than 100 of these converge onto each of about 50,000 Kenyon cells (R.A.J. and G.L., *Soc. Neurosci. Abstr.* **412**, 21, 2004). Odor identity information has been shown to be broadly distributed across the ensemble of projection cells[11,24,26]. (In the locust, the extent to which this convergence is genetically or otherwise specified is not known; by comparison, genetic labeling techniques have shown that *Drosophila* have some well-specified connectivity[40,41].)

Our analysis adhered to these features of olfactory anatomy and physiology; we used techniques that permitted us to examine the odor-elicited responses in an ensemble of more than 100 projection neurons in a series of brief time bins (**Supplementary Fig. 1**). Odorants evoked responses in most projection neurons (**Fig. 2**). Measures of the inter-response Euclidean distance (**Fig. 3**) and cross-correlation (**Fig. 4**) indicated (i) that the responses evolved gradually during and after the stimulus, (ii) that different odor concentrations evoked responses that differed from each other to some extent, and (iii) that different odorants evoked responses that differed to a greater extent. These responses were reliable over repeated trials and could be visualized as trajectories looping through a high-dimensional representation space (**Fig. 5**, **Supplementary Fig. 2**). These results confirm our earlier work[26].

Odor stimuli tend to repeat in nature because of iterative olfactory behaviors such as sniffing[42] and antennal sweeping[43] and also because of turbulence, which can deliver an odor to receptors as a series of transient encounters with odor filaments[20]. We found that, most of the time, the long, complex projection-neuron responses to each of the odor pulses within a train interfered with each other (**Fig. 1**). Yet we found no projection neurons that closely tracked trains of all odors, and thus no evidence for a specialized 'channel' for stimulus timing as exists in auditory systems. Nonetheless, when our set of 117 projection neurons was considered together, responses to multiple and rapid pulses were sufficiently correlated with one another (**Fig. 7**) to permit the odors to be accurately classified, regardless of the odor-pulse presentation pattern (**Figs. 6** and **7**). Indeed, trajectory representations of the ensemble response show largely overlapping, re-circling patterns corresponding to each odor pulse in a train (**Fig. 5**). Any given 50-ms time bin contained enough information to successfully serve as a template to classify odors (**Fig. 6**). Further, we found that single 50-ms templates taken from one presentation pattern could successfully classify responses to other presentation patterns (**Fig. 6**); thus, the olfactory system need not memorize every permutation of odor and presentation pattern in order to recognize a particular odor in the future. Additionally, by describing brief portions of odor responses, such as the response onset (as in **Fig. 6**), templates can characterize the temporal properties of the odor stimulus.

When the IPI was brief, each new ensemble response truncated the previous one, as is evident in the correlation analyses (**Figs. 4** and **7**) and trajectory representations (**Fig. 5**). This truncation left the early portion of each response largely intact. Although useful templates could be drawn from any time in the response, the onset of the response to each pulse in the train provided the most reliable across-pulse and across-pattern templates (**Fig. 6**). Notably, the most effective templates occurred about 300 ms after the ensemble response onset (**Supplementary Fig. 3**)—the earliest time at which maximal odor-identifying information is available from projection-neuron responses (see Fig. 6d in ref. 26). Thus, the circuitry of the antennal lobe seems to be largely 'reset' by each new stimulus pulse. As a result, regardless of the presentation pattern, each odor-specific ensemble response begins similarly and then follows a similar trajectory.

We observed up to 68% variability in the responses to each combination of projection neuron and odor; these responses were calculated cumulatively over either three or ten pulses. However, the response variability between any one pulse and any other was less than 68%. For example, for the series of three pulses with a 500-ms IPI, the percentages of neurons that changed their responses significantly ($P < 0.05$; see Methods) between the first and second, first and third, and second and third pulses were 26.67%, 30.1% and 22.3%, respectively. In addition, of the projection neurons that changed their responses, only 20.62% of the neurons changed their responses across all pulse pairs. Thus, considered only pair-wise (that is, between any given pulse and another), most individual projection neurons had similar responses, thus providing a foundation for extracting invariance. It is critical to note, however, that the subset of projection neurons that responded consistently for one pair of pulses was not the same as the subset that responded consistently for a different pair. For example, only 54.8% of the projection neurons that significantly changed their responses between the first and second pulses also changed their responses between the first and third pulses. Our analysis shows that the problem of response classification can be solved by the convergence of many projection neurons onto Kenyon cells. The Kenyon cells each examine a large ensemble of projection neurons, which—by virtue of its large size—will contain enough projection neurons that respond consistently to a given stimulus. The remaining highly variable responses, which could dominate a smaller ensemble (**Supplementary Fig. 4**), would be insufficient to prevent successful classification.

How large should a projection-neuron ensemble be if responses are to be classified successfully? If we assume that the connectivity between projection neurons and Kenyon cells is imprecisely specified, Kenyon cells cannot know which subset of the projection neurons will provide faithful, stimulus-tracking responses for any given odor and pulse pattern. With our set of 117 projection neurons, we achieved classification success far better than chance (**Fig. 6**). We also found, not surprisingly, that response classification deteriorated when we used successively smaller subsets of projection neurons for our analysis (**Supplementary Fig. 4**; see also Fig. 6e in ref. 26). Classification with smaller projection-neuron ensembles might be possible with more precisely specified mapping between projection neurons and Kenyon cells, experience-dependent plasticity or both.

We analyzed brief (50-ms) time bins of activity because Kenyon cells seem to sample the projection-neuron ensemble on this time scale[24]. It is not known whether neurons that succeed Kenyon cells in the olfactory pathway are able to integrate olfactory information over longer durations (as was predicted in a previous study[44]). Not surprisingly, we found that longer templates, formed by concatenating up to 20 of the 50-ms templates, marginally improved odor classification, but once the template duration exceeded the IPI of the odor train, classification deteriorated (data not shown). Thus, if the IPI is unpredictable or variable, as is the case in most natural odor plumes, brief samples of activity may be of the most general utility. A system designed to use such samples would function well when it encounters rapid trains of brief odor pulses (such as, for instance, when an odor source is distant). When odor samples are encountered at longer and more widely spaced intervals, the same system could continue to extract and memorize the additional, partially redundant information available in the longer responses—consistent with behavioral results showing that animals require more time to solve difficult olfactory tasks[45].

In Kenyon cells, the responses to odors were consistent with the information detectable by the convergence of multiple projection neurons: as previously described[26], Kenyon cells fired in response to particular odors and concentrations, and at particular times. Over the trains of odor pulses, individual Kenyon cells responded reliably at particular times to the pulses (**Fig. 8a**, KC 1,2). If a Kenyon cell responded to more than one test odorant, the response time could be different for different odorants (**Fig. 8a**, KC 3). This timing preference probably results from the transient coactivity of subgroups of projection neurons that converge onto a given Kenyon cell; through such convergence, Kenyon cells correspond to particular points along the response trajectory of the projection-neuron ensemble. As a group, Kenyon cells responded during and briefly following odor presentations, with small activity peaks for each pulse; notably, however, most responses occurred at the onset of each odor train (**Fig. 8b**). When the inter-pulse interval was brief (that is, 500 ms), Kenyon cells responded most often to the first pulse but continued to respond throughout the train. Given our relatively sparse sampling of the large Kenyon-cell population, it remains an open and interesting question why the first pulse elicited the strongest responses.

There is no behavioral evidence to suggest that locusts use information about the temporal presentation characteristics of odors. Our results, however, suggest that such timing information is available within the olfactory response. We speculate that animals would benefit from detecting and recognizing characteristic timing features of an odor plume, such as its onset, continued presence and offset; we predict that one could, for example, train animals to respond behaviorally to specific, rewarded temporal features in a complex odor sequence.

Multiple factors seem to underlie the changes in the response patterns of projection neurons and Kenyon cells over the course of a rapid train of odor pulses. In projection neurons, these factors include the cumulative superimposition of long-lasting, odor-driven excitatory and inhibitory inputs from afferent, projection and local neurons within the antennal lobe. These factors constrain the firing patterns of projection neurons and thus constitute the mechanism underlying the partial circuit reset triggered by each odor pulse. In addition, there are at least two forms of plasticity: rapid but short-lived adaptation in odor receptors (detected as decreasing EAG amplitude, **Fig. 1**); and gradual but long-lasting 'fast learning' within the lobe[46,47]. Kenyon cells are additionally influenced by feed-forward inhibition from the lateral horn[24]. We are presently exploring these mechanisms and their interactions in detail (S.L.B. and M.S., unpublished data).

METHODS

Animals. Experiments were performed on 116 intact adult locusts (*Schistocerca americana*) of both sexes from our crowded colony. Animals were immobilized and stabilized with wax; one antenna was secured intact and the other was removed and used to record an electroantennogram (see below). The brain was exposed, desheathed and superfused with locust saline as previously described[11].

Odor stimulation. Dried and activated carbon-filtered air (0.75 liter min^{-1}) flowed continuously across the antenna through a Teflon tube (6.35 mm inner diameter) placed perpendicular to and within 4 mm of the intact antenna. A large vacuum funnel was placed 10 cm behind the antenna so as to quickly remove odorants. Twenty milliliters of each liquid odorant—either neat or diluted in mineral oil (J.T. Baker)—were placed in 60-ml glass bottles; the odors, drawn from the headspace above these odorants, were puffed by a pneumatic picopump (WPI) into the continuously flowing air stream, thus further diluting the odorant. The timing of odor release was controlled by a Master-8 stimulus generator (A.M.P.I.) or by a custom computer program. The odorants used in the intracellular recordings were 1-hexanol, 1-octanol, hexanal (Fluka), geraniol (Sigma), *trans*-2-hexen-1-ol and 2-heptanone (Aldrich) as well as extracts of strawberry, cinnamon, peach, lime (Balducci's), wintergreen and Sambuca (Wagner's), used neat or dilutions of 10:1 and 100:1. For the extracellular recordings, 1-hexanol, geraniol, 1-octanol and hexanal were used neat and at 100:1 dilutions (denoted throughout the text as 1 and 0.01).

Electrophysiology. Electroantennogram recordings (EAGs) were made by inserting chlorided silver wire electrodes (0.127 mm diameter, WPI) into the cut ends of an isolated antenna. Wires were secured with small drops of wax and fed into a DC amplifier (Brownlee Precision). Intracellular recordings were made from neurons in the antennal lobe using sharp glass micropipettes (outer diameter 1.0 mm; Warner Instruments); these had been pulled with a Sutter P97 horizontal puller (Sutter Instruments) and filled with 0.5 M potassium acetate and 5% neurobiotin (Vector Laboratories) to yield resistances of 80–230 MΩ. The data were digitally acquired at a sampling rate of 5 kHz (LabView software; PCI-6602 DAQ and PCI-MIO-16E-4 hardware, National Instruments) and stored on a PC hard drive; they were then analyzed off-line using MATLAB (MathWorks).

Multiunit recordings from the projection neurons were made using 16-channel, 4 × 4 silicon probes (NeuroNexus Technologies) and from the Kenyon cells using custom-made twisted wire tetrodes[24] with a 16-channel DC amplifier (Biology Electronics Shop, Caltech). The data were digitally sampled at 15 kHz. Multiunit projection-neuron and Kenyon-cell spike sorting was achieved offline by a four-wire, whole-waveform algorithm (Spike-O-Matic[48]) implemented in Igor (Wavemetrics). Spike sorting was conservative: we analyzed only those clusters that were unambiguously defined and clearly separated from one another throughout the experiment. The criteria we used to select these clusters included the following: (i) nearest cluster projections had to lie at least 5 standard deviations (s.d.) apart, (ii) no more than 2% of the ISIs were under 20 ms and (iii) the waveform s.d. could not exceed 5%. These criteria are described elsewhere[48].

Analysis. All analyses were performed using custom programs in MATLAB. To determine whether the odor-elicited spike numbers changed significantly with pulse position, we used the following algorithm: (i) we evaluated whether a particular combination of odor and projection neuron elicited spikes—defined as an increase over the baseline firing rate by 6.5 s.d., in any post-stimulus 50-ms bin (this procedure yielded response detection that closely matched an observer's judgments); (ii) we then performed a two-way analysis of variance (ANOVA) on the spike counts obtained, over ten repeated trials, during the 500 ms after each pulse.

To analyze the response of the projection-neuron ensemble (117 projection neurons) over time, we constructed a series of 117-dimensional vectors, each representing the ensemble's firing during a single 50- or 100-ms time bin; each vector element consisted of the number of spikes in a single projection neuron during the time bin. We refer to these vectors as snapshots, as they represent the ensemble response at a moment in time.

Beginning at 2 s before the first odor pulse, we collected data for a total of 15 s; then, to measure the Euclidean distance between ensemble response vectors, these data were binned into 50-ms time bins. The Euclidean distance for one group (that is, all trials, odors or concentrations) is given by the average across all pairs within the group. For two groups, the distance is given by the average across all pairs from the two groups.

The cross-correlations between the response vectors were computed for each combination of time bins in the ensemble response as follows: if $\mathbf{x}$ is the 117-dimensional vector representing the response to a given odor, then for the i^{th} trial, $\mathbf{x}(i)$, the cross-correlation between the responses at times k and l (that is, $\mathbf{x}_k(i)$ and $\mathbf{x}_l(i)$) is calculated as

$$\left(\sum_{i=1}^{10} \boldsymbol{x}_k^{\mathrm{T}}(i)\boldsymbol{x}_l(i)\right) \Big/ \left(\left(\sum_{i=1}^{10} \boldsymbol{x}_k^{\mathrm{T}}(i)\boldsymbol{x}_k(i)\right)\left(\sum_{i=1}^{10} \boldsymbol{x}_l^{\mathrm{T}}(i)\boldsymbol{x}_l(i)\right)\right)^{1/2}$$

We then averaged across odors to get the cross-correlation at the $(k,l)^{th}$ point in the plot. Estimates were made using ten trials, and only correlations with significance of $P < 0.001$ (t-test) are shown.

For nonlinear dimensionality reduction with locally linear embedding (LLE)[28], we used code from S. Roweis (http://www.cs.toronto.edu/~roweis/lle). The LLE method first finds a linear transformation, invariant to rotation and scaling, that represents each point in terms of each of its neighbors. Then a representation with reduced dimensionality is calculated by estimating a new set of points that satisfies the above transformation with respect to all the points. When applied to our data, principal component analysis (PCA) yielded results that were qualitatively similar to those from LLE, but—because our high-dimensional data were not well described by linear functions—LLE characterized and separated the response trajectories more effectively. The input to LLE consisted of the 117-dimensional snapshot vectors, each 100-ms wide and averaged over three trials. Qualitatively similar results were obtained using 50-ms time bins. LLE was calculated for the four different pulse sequences jointly and later plotted on separate, matching axes. LLE gave qualitatively similar results for a wide range of neighborhood values (between 10 and 20), indicating the genuine presence of low-dimensional manifolds that are well characterized by this analysis.

For the classification analysis, we used the 50-ms time bins. The high dimensionality of our dataset could permit spurious over-classification of odors; to avoid this, we first reduced the dimensionality of our dataset using PCA. For classification based on templates, we applied the k-means function in MATLAB to the first eight dimensions in our dataset. Our choice of eight dimensions (which together contributed 32% of the variance) was based on standard practice: we identified the elbow in a scree plot of our eigenvalues[49]. Neighbors were decided on the basis of the Euclidean distance. For template-based classification, the templates were the centroids of ten repeated trials. To estimate the confidence level of our template-based classification, a histogram of the percentage of template-based classification was calculated from ensemble activity at times before the odors were presented; the probability of obtaining >30% classification success in the absence of a stimulus was <0.002 (**Supplementary Fig. 5**).

We pooled projection neurons sampled from 14 experiments to approximate a single, large (technically unfeasible) recording from a single animal. This raises the possibility of including in our set multiple examples of the same projection neuron from different animals. However, an inspection of the odor responses of our 117 projection neurons suggested that no duplicates existed. Further, we performed a 10,000-iteration Monte Carlo simulation of our sampling process with the same numbers of projection neurons (between 3 and 17) and animals (14) as in our data. Results showed a non-zero, but very small, probability for the duplication of any projection neuron (see **Supplementary Fig. 6**; for a discussion of this issue, see ref. 26).

Note: Supplementary information is available on the Nature Neuroscience website.

ACKNOWLEDGMENTS

We are grateful to members of the Stopfer lab for helpful discussions. This work was funded by an intramural grant from the National Institutes of Health, the National Institute of Child Health and Human Development.

COMPETING INTERESTS STATEMENT

The authors declare that they have no competing financial interests.

Published online at http://www.nature.com/natureneuroscience/
Reprints and permissions information is available online at http://npg.nature.com/reprintsandpermissions/

1. Fuster, J.M. & Jervey, J.P. Neuronal firing in the inferotemporal cortex of the monkey in a visual memory task. *J. Neurosci.* **2**, 361–375 (1982).
2. Richmond, B.J., Optican, L.M., Podell, M. & Spitzer, H. Temporal encoding of two-dimensional patterns by single units in primate inferior temporal cortex. I. Response characteristics. *J. Neurophysiol.* **57**, 132–146 (1987).

3. McClurkin, J.W., Optican, L.M., Richmond, B.J. & Gawne, T.J. Concurrent processing and complexity of temporally encoded neuronal messages in visual perception. *Science* **253**, 675–677 (1991).
4. Meister, M. Multineuronal codes in retinal signaling. *Proc. Natl. Acad. Sci. USA* **93**, 609–614 (1996).
5. Nagarajan, S.S. *et al.* Representation of spectral and temporal envelope of twitter vocalizations in common marmoset primary auditory cortex. *J. Neurophysiol.* **87**, 1723–1737 (2002).
6. Gehr, D.D., Komiya, H. & Eggermont, J.J. Neuronal responses in cat primary auditory cortex to natural and altered species-specific calls. *Hear. Res.* **150**, 27–42 (2000).
7. Machens, C.K. *et al.* Representation of acoustic communication signals by insect auditory receptor neurons. *J. Neurosci.* **21**, 3215–3227 (2001).
8. Jones, L.M., Depireux, D.A., Simons, D.J. & Keller, A. Robust temporal coding in the trigeminal system. *Science* **304**, 1986–1989 (2004).
9. Arabzadeh, E., Zorzin, E. & Diamond, M.E. Neuronal encoding of texture in the whisker sensory pathway. *PLoS Biol.* **3**, E17 (2005).
10. Jones, L.M., Lee, S., Trageser, J.C., Simons, D.J. & Keller, A. Precise temporal responses in whisker trigeminal neurons. *J. Neurophysiol.* **92**, 665–668 (2004).
11. Laurent, G. & Davidowitz, H. Encoding of olfactory information with oscillating neural assemblies. *Science* **265**, 1872–1875 (1994).
12. Hamilton, K.A. & Kauer, J.S. Responses of mitral/tufted cells to orthodromic and antidromic electrical stimulation in the olfactory bulb of the tiger salamander. *J. Neurophysiol.* **59**, 1736–1755 (1988).
13. Meredith, M. Patterned response to odor in mammalian olfactory bulb: the influence of intensity. *J. Neurophysiol.* **56**, 572–597 (1986).
14. Laurent, G., Wehr, M. & Davidowitz, H. Temporal representations of odors in an olfactory network. *J. Neurosci.* **16**, 3837–3847 (1996).
15. Wehr, M. & Laurent, G. Odour encoding by temporal sequences of firing in oscillating neural assemblies. *Nature* **384**, 162–166 (1996).
16. Lestienne, R. Spike timing, synchronization and information processing on the sensory side of the central nervous system. *Prog. Neurobiol.* **65**, 545–591 (2001).
17. Theunissen, F. & Miller, J.P. Temporal encoding in nervous systems: a rigorous definition. *J. Comput. Neurosci.* **2**, 149–162 (1995).
18. Laurent, G., MacLeod, K., Stopfer, M. & Wehr, M. Dynamic representation of odours by oscillating neural assemblies. *Entomol. Exp. Appl.* **91**, 7–18 (1999).
19. Laurent, G. A systems perspective on early olfactory coding. *Science* **286**, 723–728 (1999).
20. Murlis, J. & Jones, C.D. Fine-scale structure of odor plumes in relation to insect orientation to distant pheromone and other attractant sources. *Physiol. Entomol.* **6**, 71–86 (1981).
21. Hildebrand, J.G. & Shepherd, G.M. Mechanisms of olfactory discrimination: Converging evidence for common principles across phyla. *Annu. Rev. Neurosci.* **20**, 595–631 (1997).
22. Wehr, M. & Laurent, G. Relationship between afferent and central temporal patterns in the locust olfactory system. *J. Neurosci.* **19**, 381–390 (1999).
23. Bazhenov, M. *et al.* Model of cellular and network mechanisms for odor-evoked temporal patterning in the locust antennal lobe. *Neuron* **30**, 569–581 (2001).
24. Perez-Orive, J. *et al.* Oscillations and sparsening of odor representations in the mushroom body. *Science* **297**, 359–365 (2002).
25. Laurent, G. & Naraghi, M. Odorant-induced oscillations in the mushroom bodies of the locust. *J. Neurosci.* **14**, 2993–3004 (1994).
26. Stopfer, M., Jayaraman, V. & Laurent, G. Intensity versus identity coding in an olfactory system. *Neuron* **39**, 991–1004 (2003).
27. Murlis, J., Elkinton, J.S. & Carde, R.T. Odor plumes and how insects use them. *Annu. Rev. Entomol.* **37**, 505–532 (1992).
28. Roweis, S.T. & Saul, L.K. Nonlinear dimensionality reduction by locally linear embedding. *Science* **290**, 2323–2326 (2000).
29. Bau, J., Justus, K.A. & Carde, R.T. Antennal resolution of pulsed pheromone plumes in three moth species. *J. Insect Physiol.* **48**, 433–442 (2002).
30. Barrozo, R.B. & Kaissling, K.E. Repetitive stimulation of olfactory receptor cells in female silkmoths Bombyx mori L. *J. Insect Physiol.* **48**, 825–834 (2002).
31. Marion-Poll, F. & Tobin, T.R. Temporal coding of pheromone pulses and trains in Manduca sexta. *J. Comp. Physiol. A* **171**, 505–512 (1992).
32. Lemon, W. & Getz, W. Temporal resolution of general odor pulses by olfactory sensory neurons in American cockroaches. *J. Exp. Biol.* **200**, 1809–1819 (1997).
33. Lei, H. & Hansson, B.S. Central processing of pulsed pheromone signals by antennal lobel neurons in the male moth *Agrotis segetum*. *J. Neurophysiol.* **81**, 1113–1122 (1999).
34. Heinbockel, T., Christensen, T.A. & Hildebrand, J.G. Temporal tuning of odor responses in pheromone-responsive projection neurons in the brain of the sphinx moth *Manduca sexta*. *J. Comp. Neurol.* **409**, 1–12 (1999).
35. Vickers, N.J., Christensen, T.A., Baker, T.C. & Hildebrand, J.G. Odour-plume dynamics influence the brain's olfactory code. *Nature* **410**, 466–470 (2001).
36. Vickers, N.J., Christensen, T.A. & Hildebrand, J.G. Combinatorial odor discrimination in the brain: attractive and antagonist odor blends are represented in distinct combinations of uniquely identifiable glomeruli. *J. Comp. Neurol.* **400**, 35–56 (1998).
37. Willis, M.A. & Avondet, J.L. Odor-modulated orientation in walking male cockroaches *Periplaneta americana*, and the effects of odor plumes of different structure. *J. Exp. Biol.* **208**, 721–735 (2005).
38. Justus, K.A. & Carde, R.T. Flight behaviour of males of two moths, *Cadra cautella* and *Pectinophora gossypiella*, in homogeneous clouds of pheromone. *Physiol. Entomol.* **27**, 67–75 (2002).
39. Lemon, W.C. & Getz, W.M. Rate code input produces temporal code output from cockroach antennal lobes. *Biosystems* **58**, 151–158 (2000).
40. Jefferis, G.S. *et al.* Developmental origin of wiring specificity in the olfactory system of *Drosophila*. *Development* **131**, 117–130 (2004).
41. Ramaekers, A. *et al.* Glomerular maps without cellular redundancy at successive levels of the *Drosophila* larval olfactory circuit. *Curr. Biol.* **15**, 982–992 (2005).
42. Fontanini, A., Spano, P. & Bower, J.M. Ketamine-xylazine-induced slow (<1.5 Hz) oscillations in the rat piriform (olfactory) cortex are functionally correlated with respiration. *J. Neurosci.* **23**, 7993–8001 (2003).
43. Okada, J. & Toh, Y. Spatio-temporal patterns of antennal movements in the searching cockroach. *J. Exp. Biol.* **207**, 3693–3706 (2004).
44. Nowotny, T., Rabinovich, M.I., Huerta, R. & Abarbanel, H.D. Decoding temporal information through slow lateral excitation in the olfactory system of insects. *J. Comput. Neurosci.* **15**, 271–281 (2003).
45. Abraham, N.M. *et al.* Maintaining accuracy at the expense of speed: stimulus similarity defines odor discrimination time in mice. *Neuron* **44**, 865–876 (2004).
46. Bazhenov, M., Stopfer, M., Sejnowski, T.J. & Laurent, G. Fast odor learning improves reliability of odor responses in the locust antennal lobe. *Neuron* **46**, 483–492 (2005).
47. Stopfer, M. & Laurent, G. Short-term memory in olfactory network dynamics. *Nature* **402**, 664–668 (1999).
48. Pouzat, C., Mazor, O. & Laurent, G. Using noise signature to optimize spike-sorting and to assess neuronal classification quality. *J. Neurosci. Methods* **122**, 43–57 (2002).
49. Joliffe, I.T. *Principal Component Analysis* (Springer-Verlag, New York, 1986).